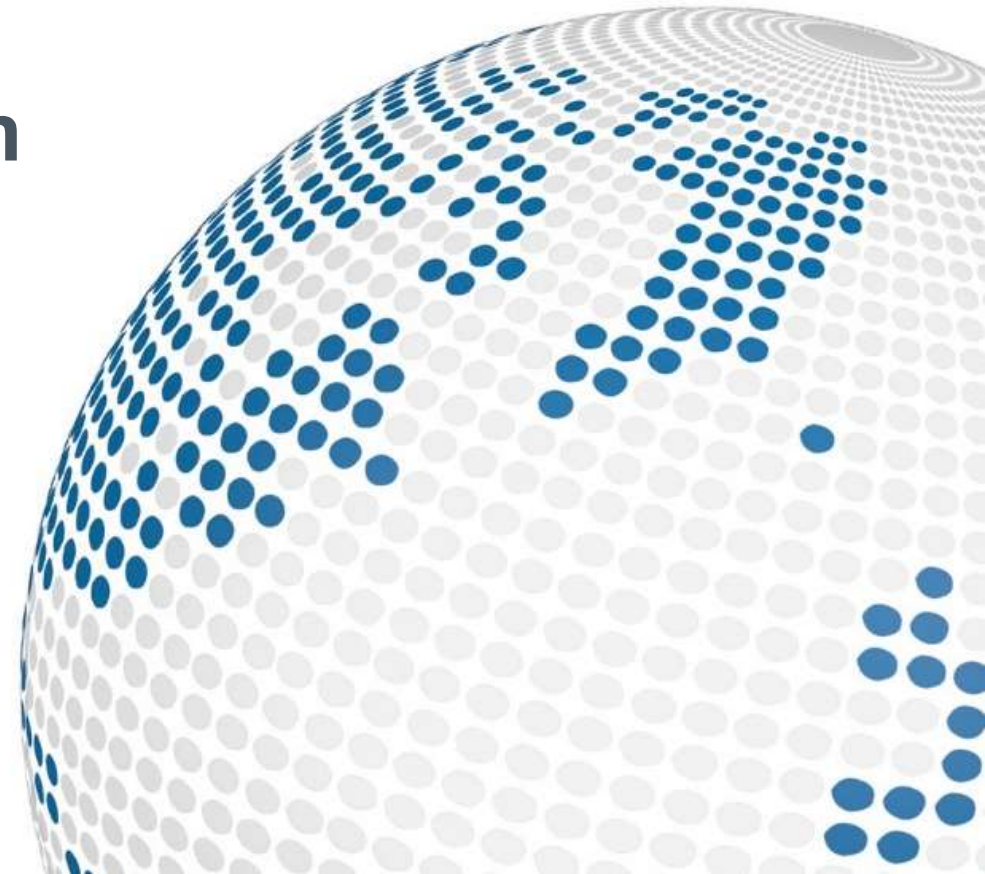


3D-Stacked SPAD in 40/45nm BSI Technology

Shaping the world with sensor solutions

Georg Röhler
June 8, 2020



Outline of Presentation

Motivation for 3D-Stacking

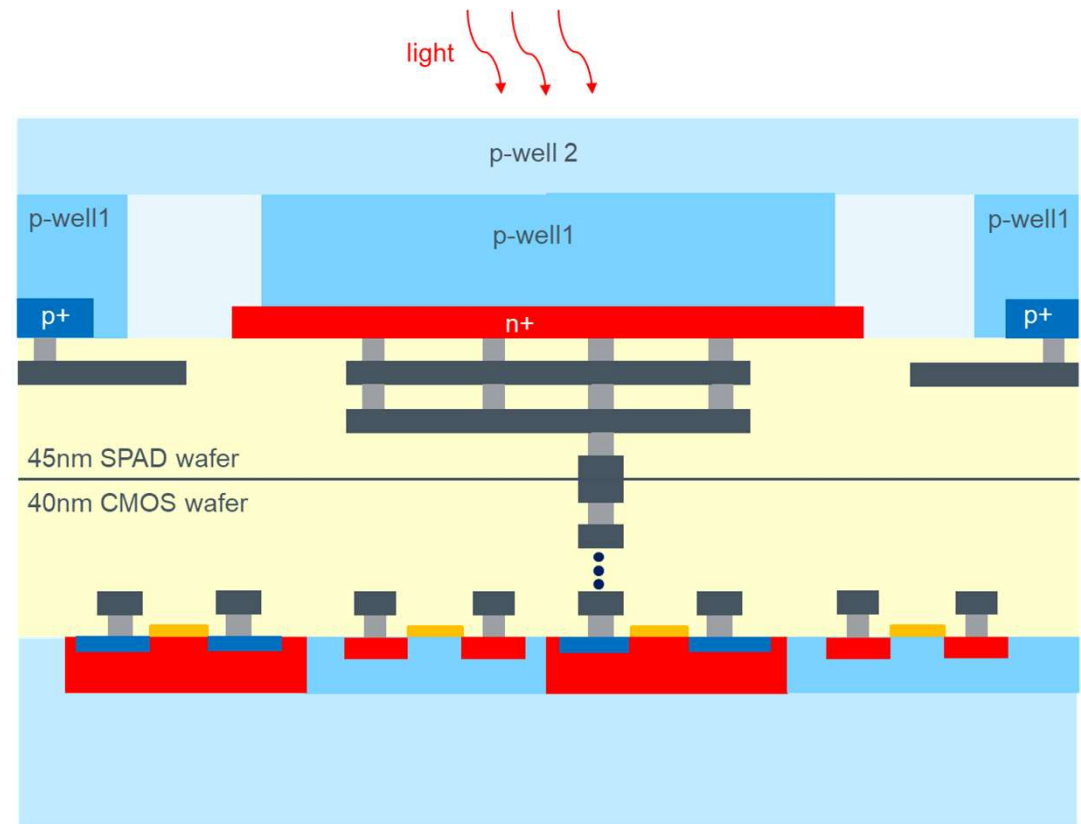
Test structure and SPAD description

Characterization Results

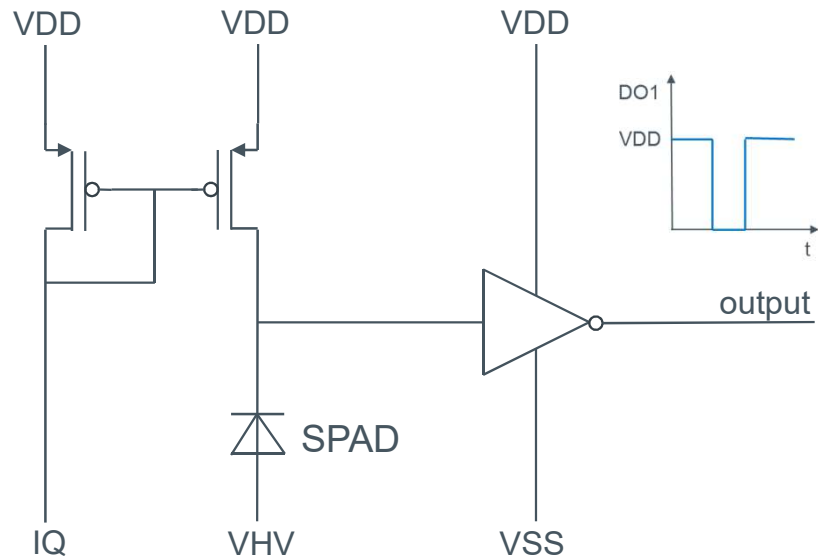
Benchmark

Motivation for 3D Stacking

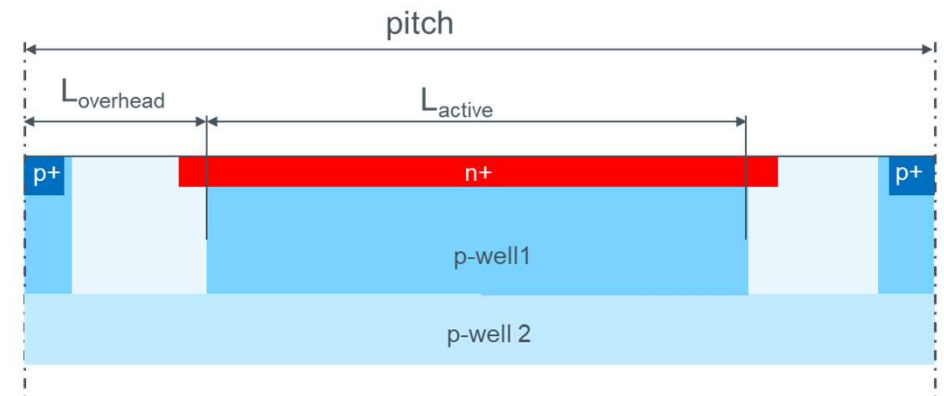
- Back side illuminated (BSI)
- Fill factor limited by SPAD only.
- Process for SPAD wafer can be optimized for SPAD performance (e.g. depletion layer width).
- SPAD process can be re-used for different CMOS nodes – enabling optimized products in terms of performance and cost.



Test Structure and SPAD Schematic



- SPAD is biased between VDD and VHV (negative).
- Passive quenching used.
- Current IQ used to set the dead time over a wide range (~10ns....~10μs).
- For crosstalk characterization, outputs for two neighboring SPADs are available.

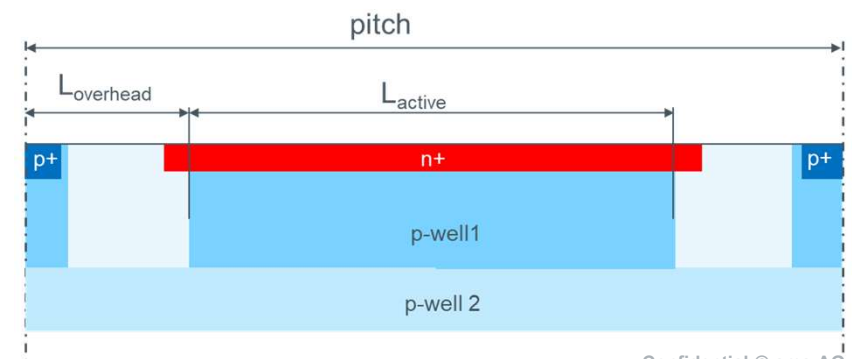
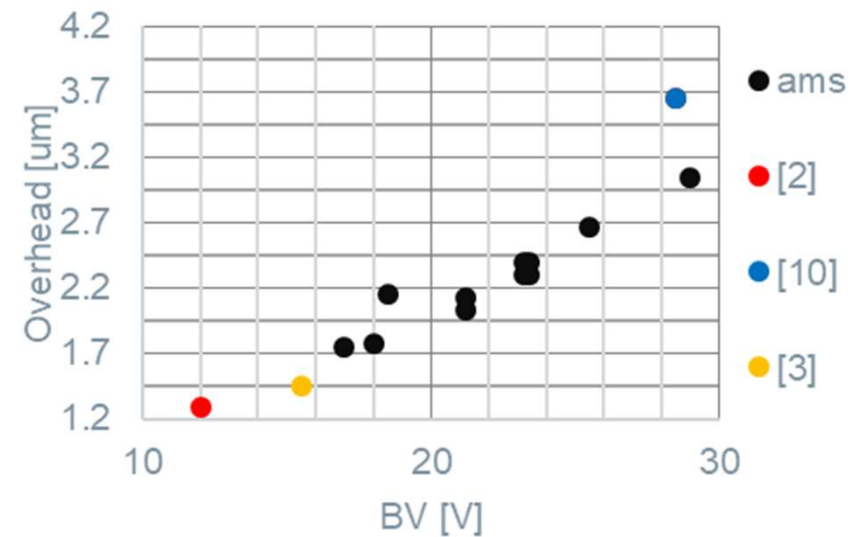


Device	Fill Factor[%]	L_{overhead} [um]
1	25	3.15
2	32	2.75
3	36	2.55
4	40	2.35
5	44	2.15
6	48	1.95
7	52	1.75

Breakdown Voltage

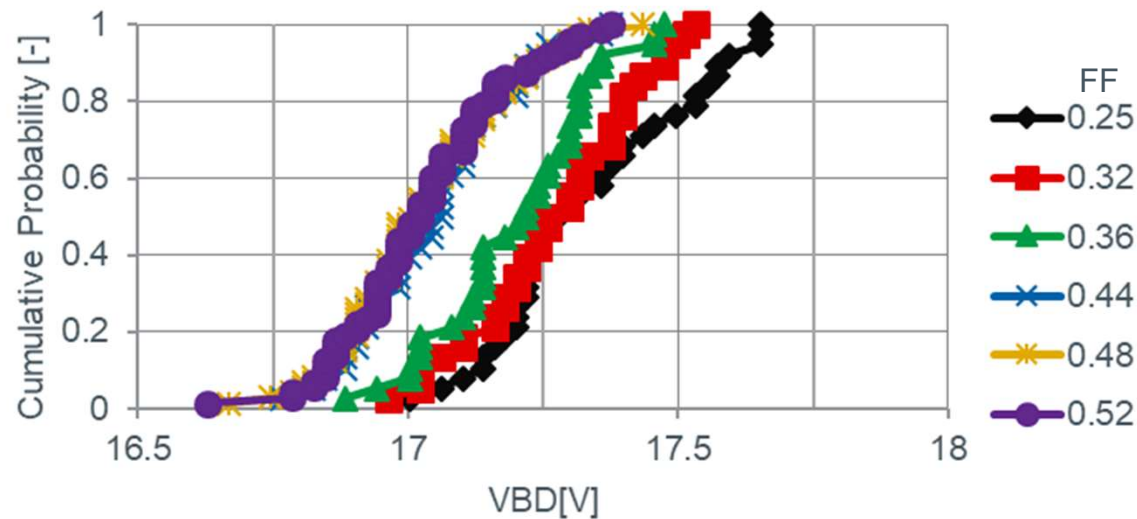
Main impact factors of breakdown voltage:

- Achievable fill factor limited by break down voltage. Required minimum “overhead” region scales approximately linearly with breakdown voltage.
- Depletion layer width (impact on PDE, junction capacitance)
- DCR (for low BV, tunneling dominates DCR).
- Energy per SPAD event scales with breakdown voltage.

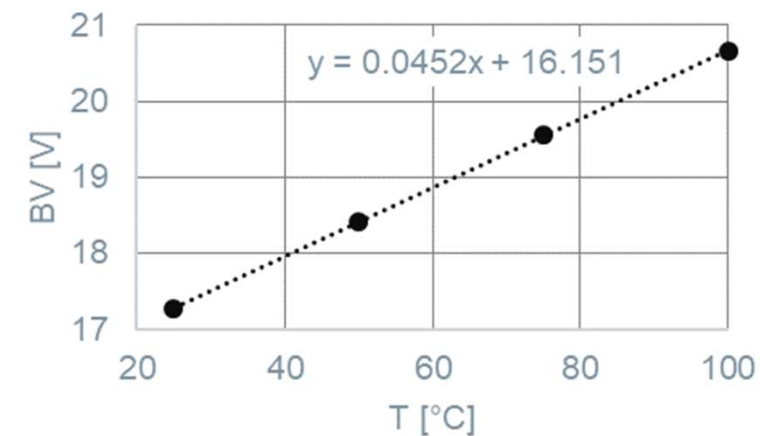
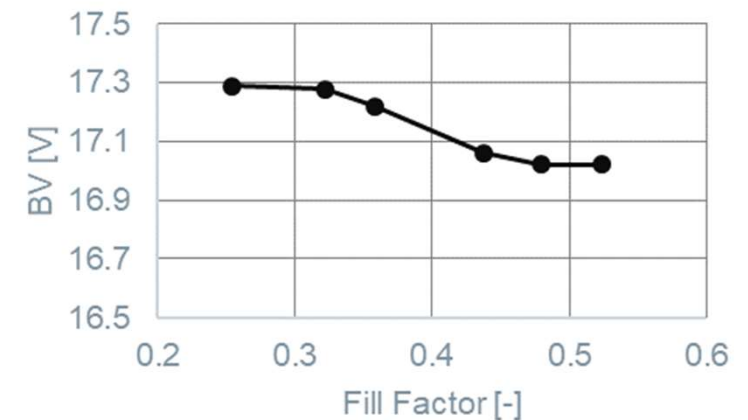


Breakdown Voltage (VBD)

Results for different fill factors

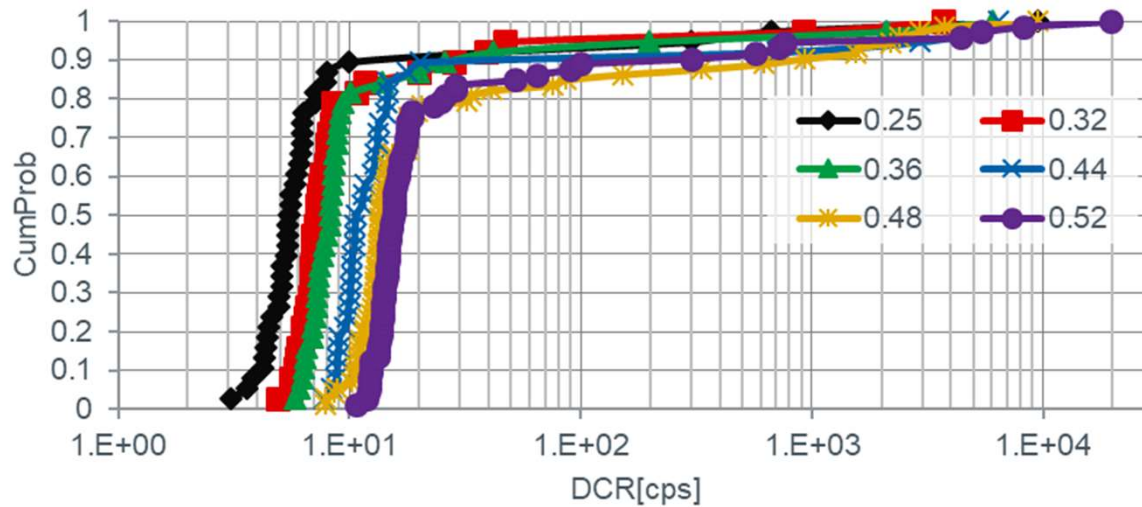


- VBD slightly decreases with fill factor (250mV).
- Standard deviation of within wafer distribution is ~150mV.
- VBD temperature coefficient is 45mV/°C, no impact of the fill factor.

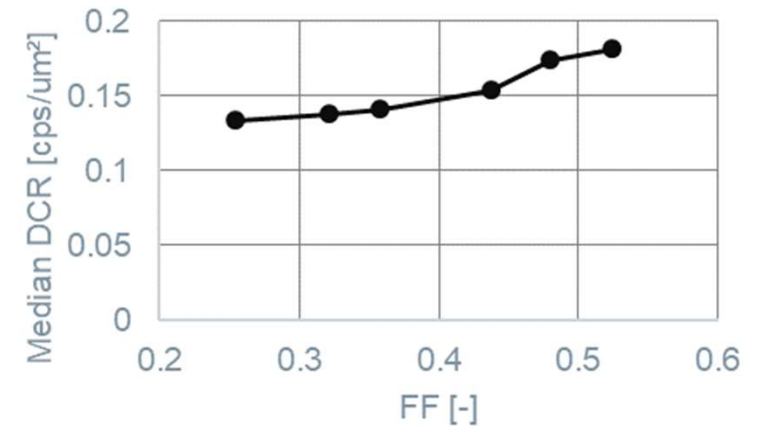
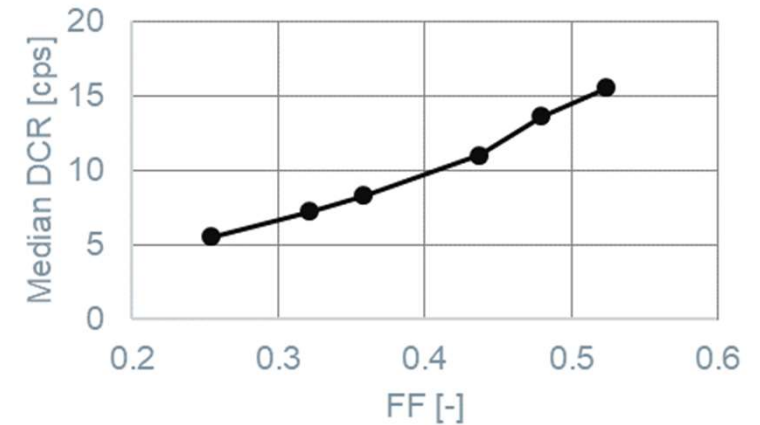


Dark Count Rate

25°C, $V_{exc}=2.0V$

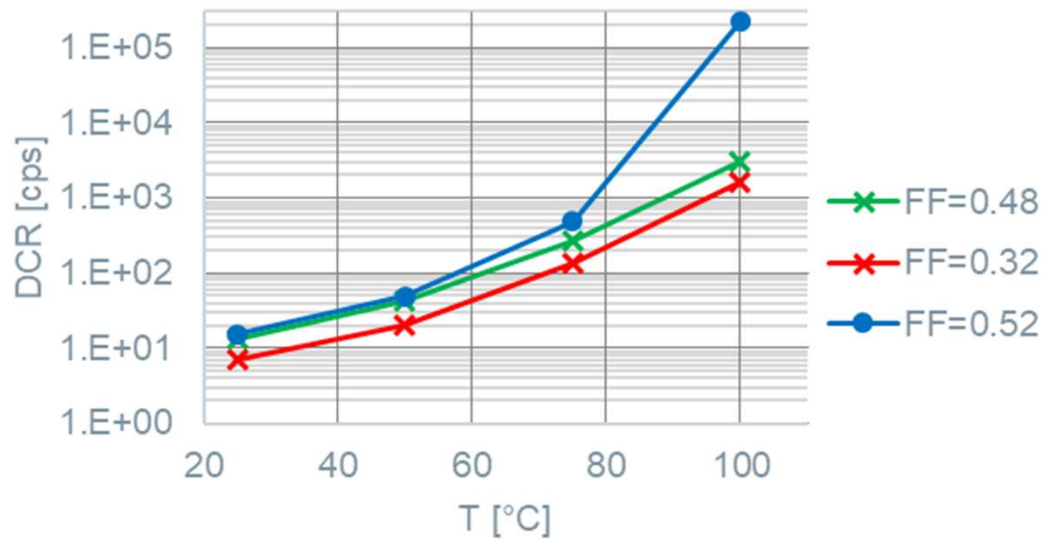


- DCR (median) is 6cps for a fill factor of 25% and 16cps for a drawn fill factor of 52%.
- Around 80% of SPADs show a DCR close to median value.
- When DCR is normalized to drawn active area, DCR (in cps/ μm^2) still increases with fill factor. Indication that drawn active area \neq real active area.

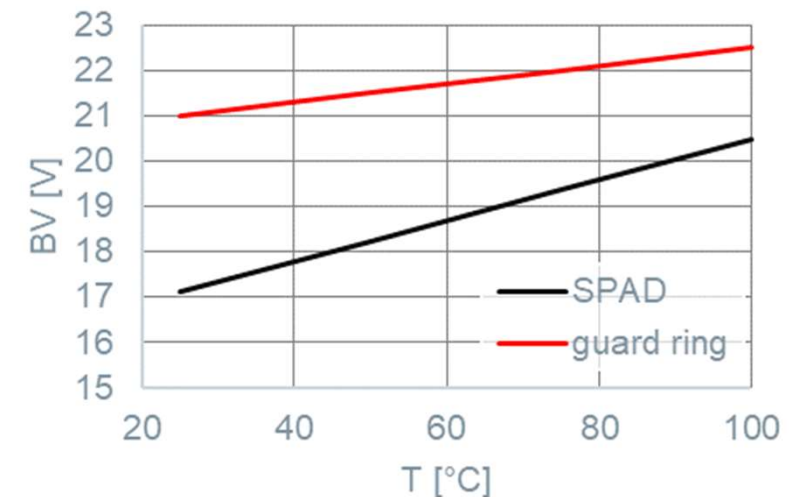
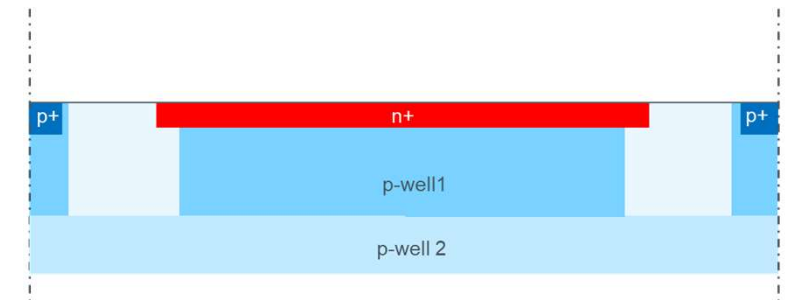


Dark Count Rate: Temperature Impact

$V_{exc}=2.0V$

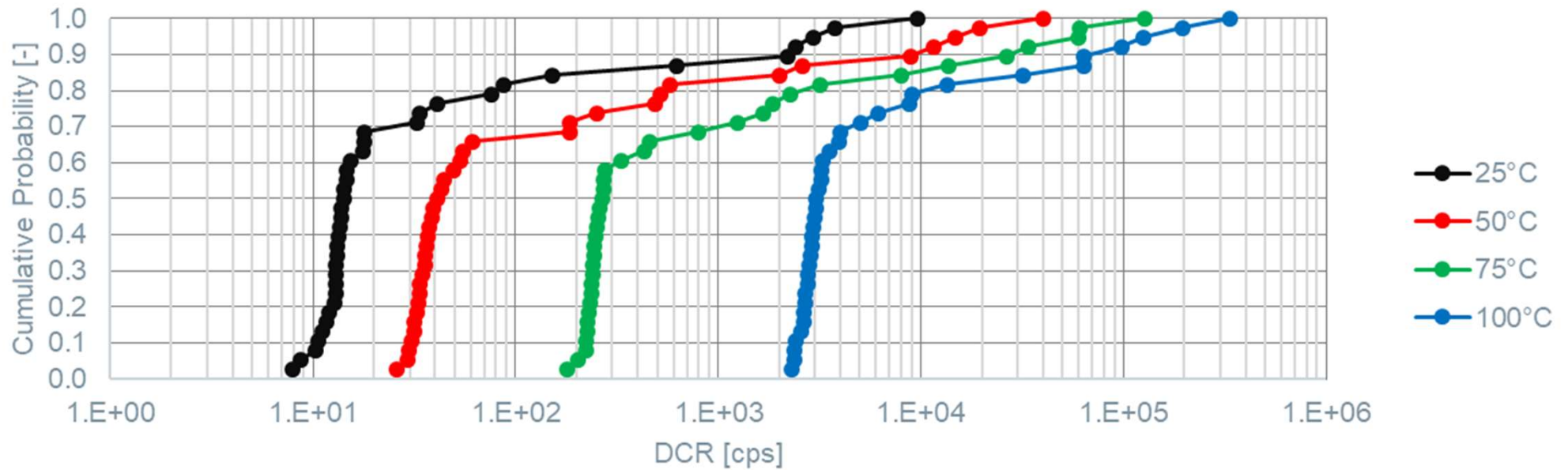


- Activation energy (extracted from 75°C and 100°C measurements) is 1.08eV.
- For the device with the fill factor of 52%, the DCR becomes very high at 100°C, caused by the different temperature coefficient of the guard ring versus the avalanche junction.



DCR Distribution for 25/50/75/100°C

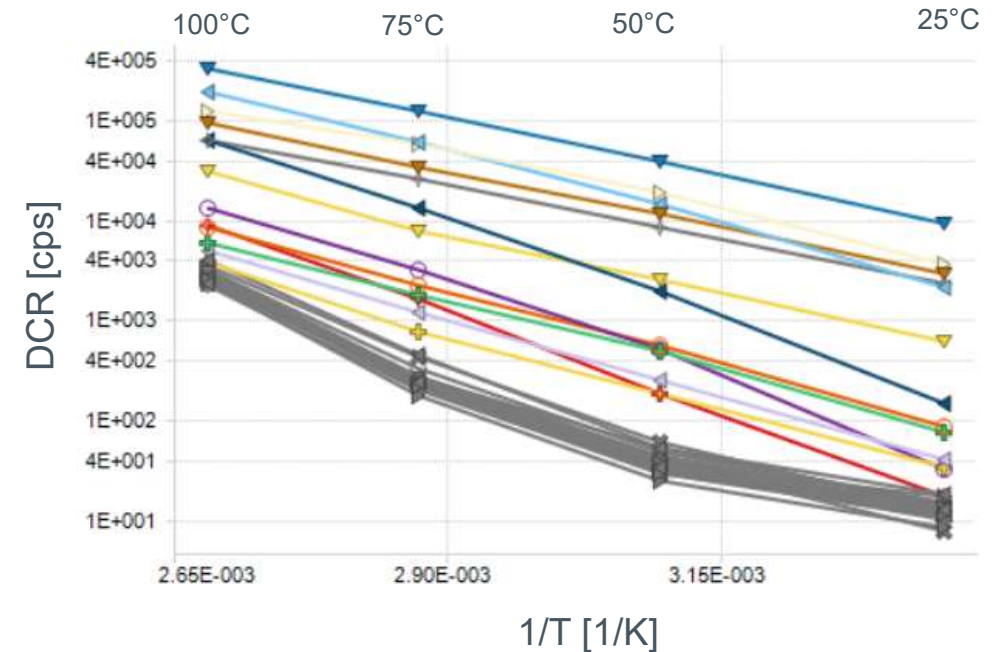
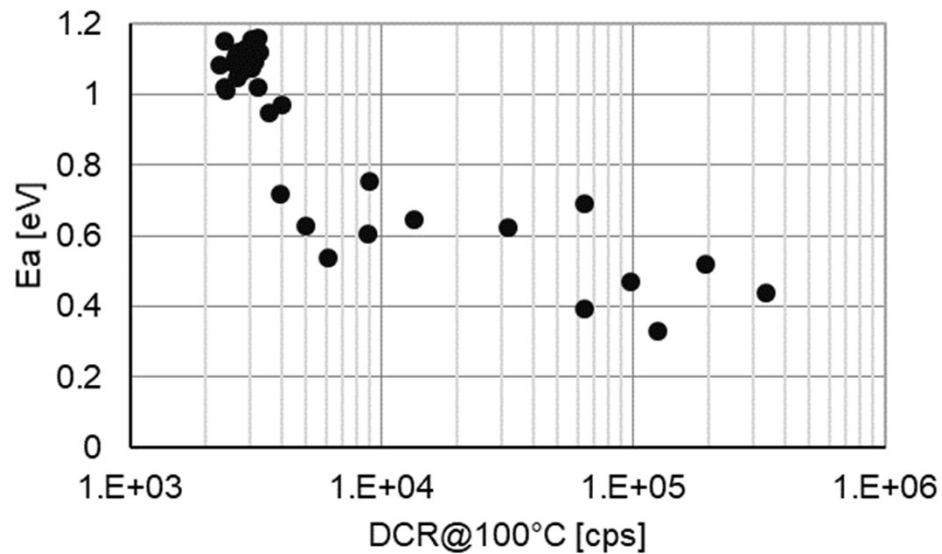
FF=0.48, V_{exc}=2.0V



- At 75°C, median DCR is 270cps and the most noisy SPAD has a DCR of 130kcps. This is still a reasonable DCR at 75°C!

Activation Energy for Hot Pixels

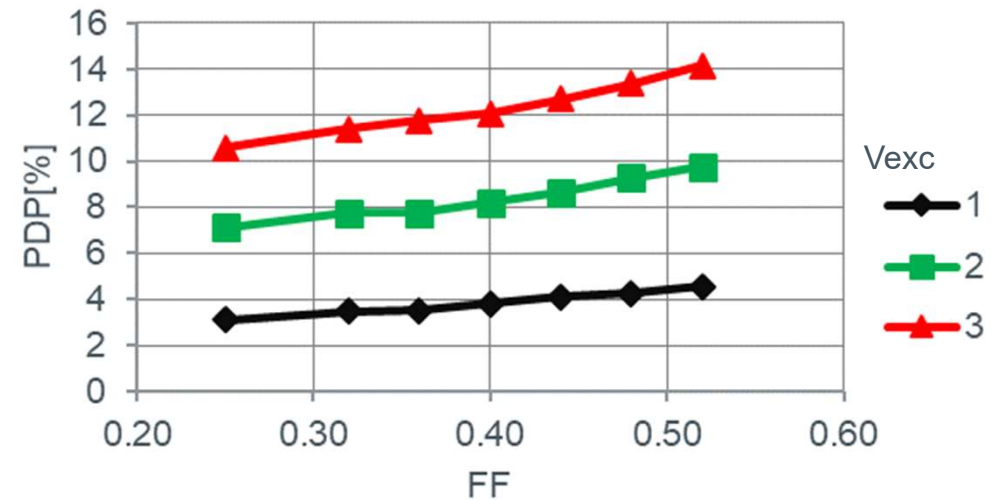
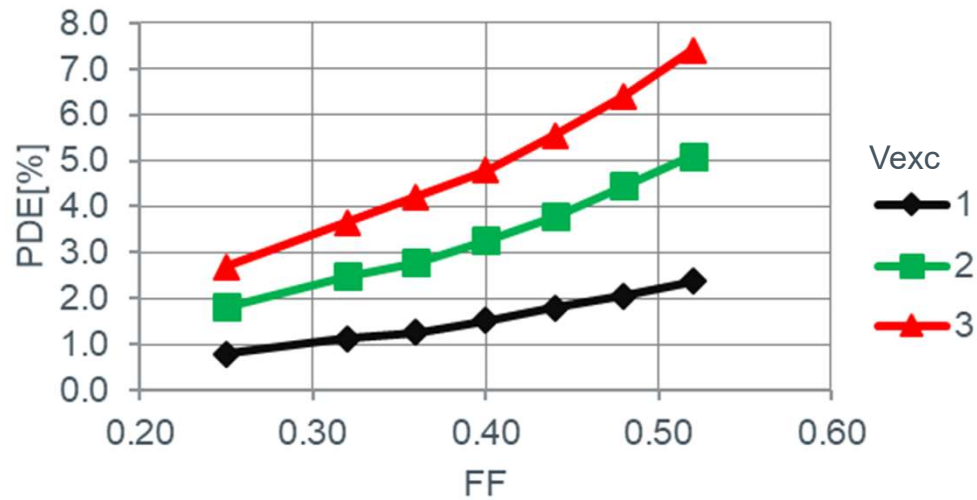
FF=0.48



- DCR for 25°C, 50°C dominated by tunneling, for 75°C and 100°C by thermal diffusion.
- Noisy SPADs dominated by diffusion for all temperatures (25°C-100°C).
- Some SPADs are in the main population at 25°C, but end up as hot pixel at 100°C and vice versa.
- Activation energy tends to be lower for SPADs with larger DCR.

Impact of Fill Factor on PDE and PDP

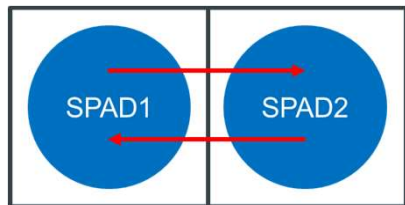
940nm



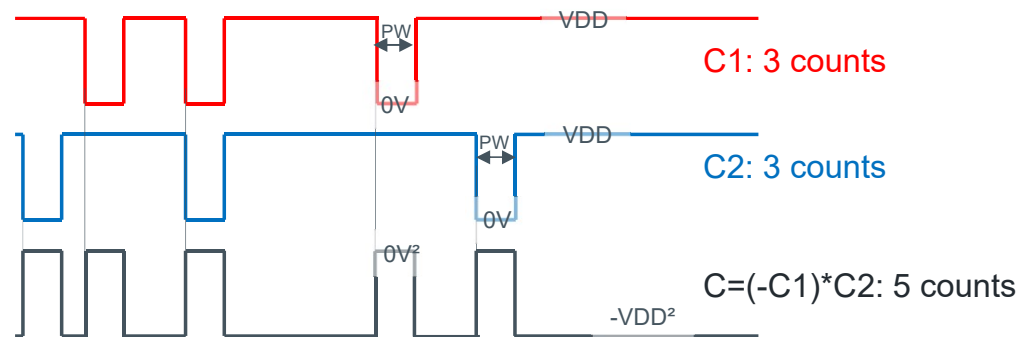
- $PDE = PDP * FF$
- PDE increases non-linearly with fill factor.
- Hence PDP is not constant over fill factor.

Crosstalk

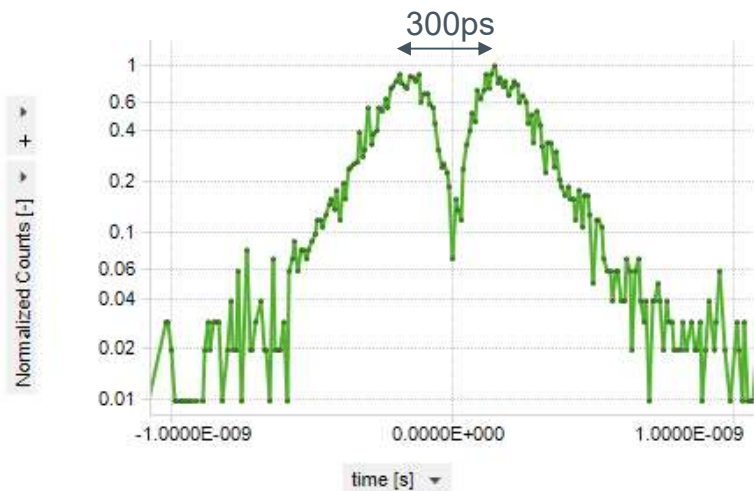
Measurement Method



Light emission of SPAD1 (when triggered by DCR or light) can trigger the neighboring SPAD2 (or vice versa) → optical orthogonal cross-talk.



The cross talk between SPAD1 and SPAD2 is measured by counting the events for SPAD1, SPAD2 and both SPADs combined. Cross talk is calculated as: $(C1+C2-C)/C$



Impact of Fill Factor and Vexc on Crosstalk (1)

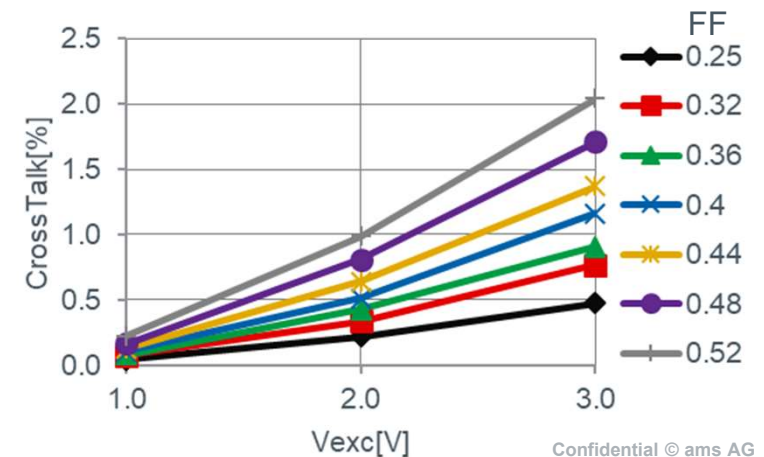
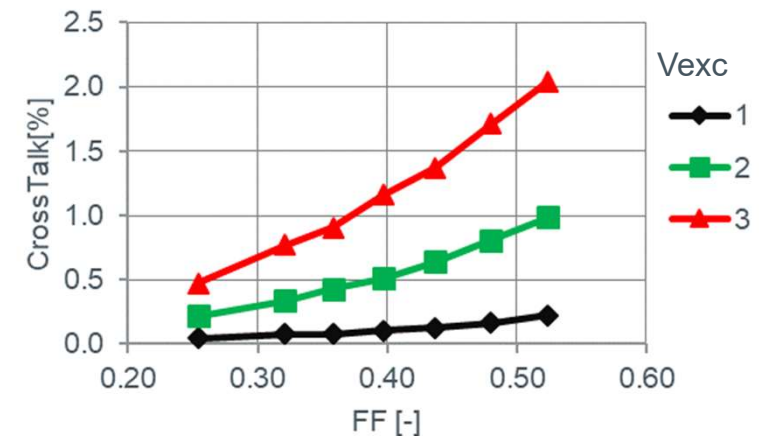
Cross talk increases with fill factor and excess bias voltage.

Fill factor:

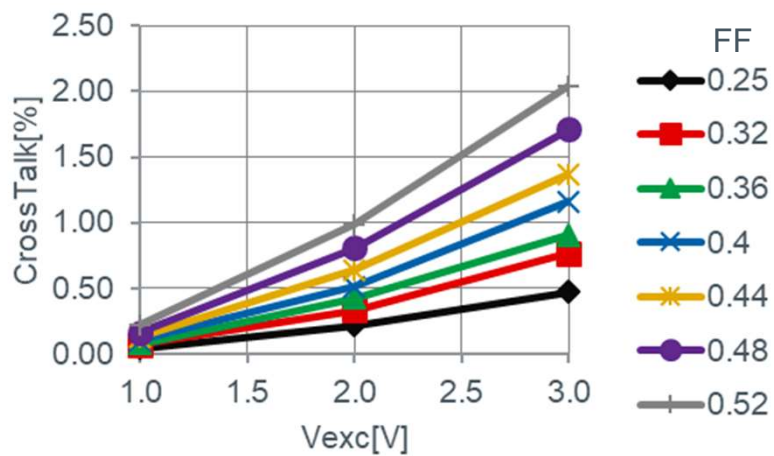
- Distance between SPAD active area becomes smaller for larger fill factors.
- Capacitance increases with fill factor, thus the charge per SPAD trigger event is increased (more light emission).
- PDE increases with fill factor.

Excess bias voltage:

- PDE increases ~linearly with excess bias voltage. Thus probability of SPAD triggering is increased.
- The charge per SPAD trigger event increases with excess bias voltage (more light emission).



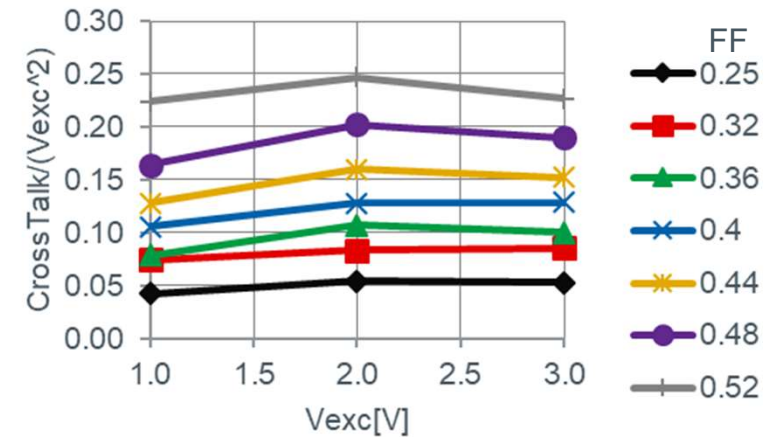
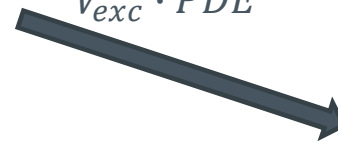
Impact of Fill Factor and Vexc on Crosstalk (2)



$$\frac{CrossTalk}{V_{exc} \cdot V_{exc}}$$

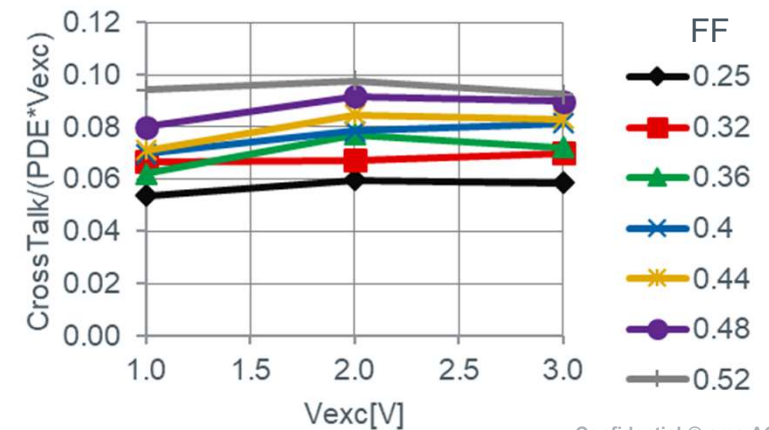


$$\frac{CrossTalk}{V_{exc} \cdot PDE}$$

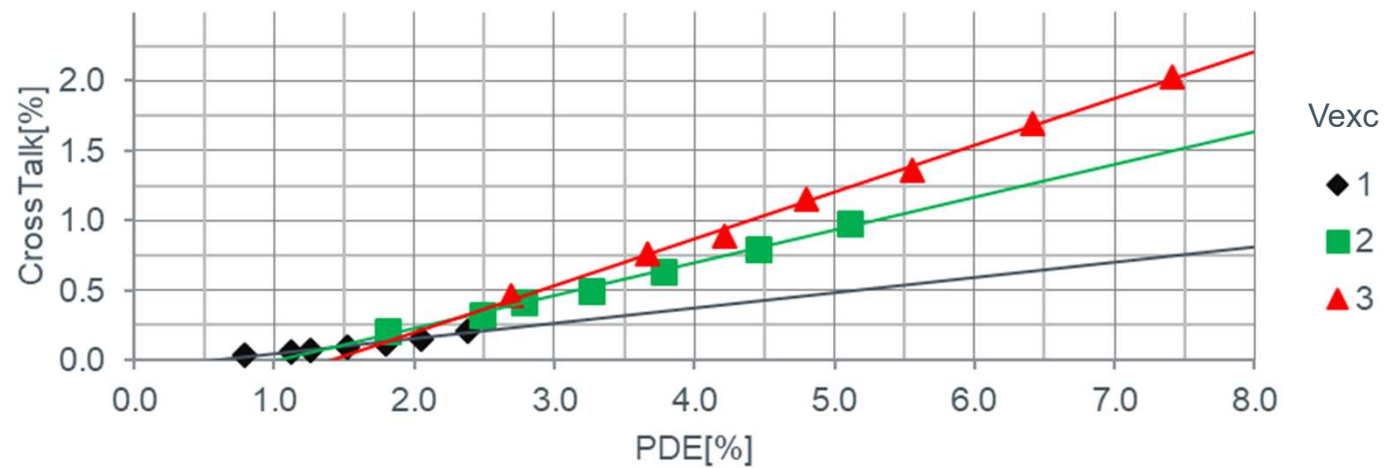


Results:

- Excess bias voltage impact nearly eliminated (less than 10% variation over Vexc remains).
- Normalization with V_{exc}^{-2} : Remaining impact of the fill factor is much stronger, since increase of PDE with fill factor is not taken into account.
- Normalization with $V_{exc} \cdot PDE$: Remaining impact of fill factor due to reduced spacing with fill factor and increased capacitance.



Crosstalk – PDE Trade-Off



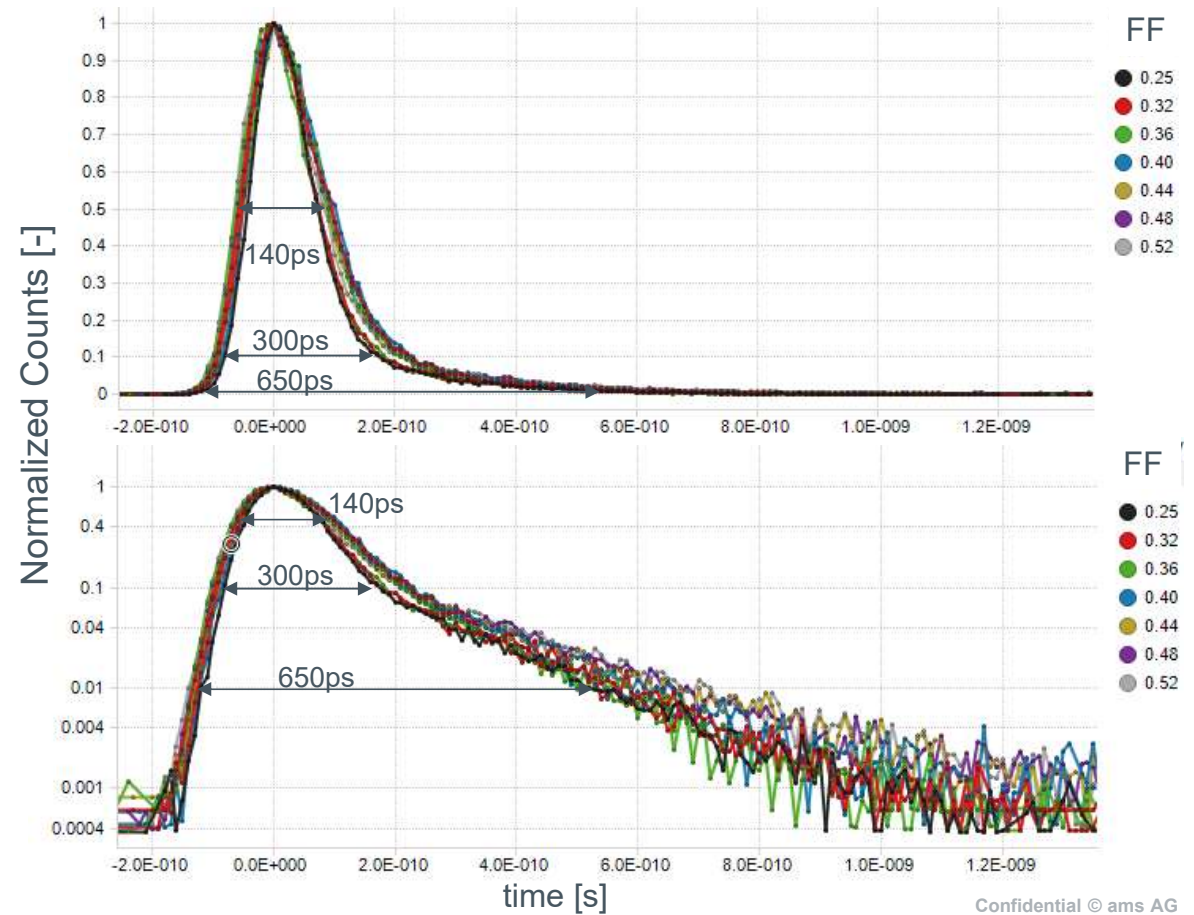
- Trade-off between PDE (@940nm) and cross-talk.
- Slightly worse trade off for larger excess bias voltage.

Timing Jitter @940nm

25°C, V_{exc}=2.0V, 940nm

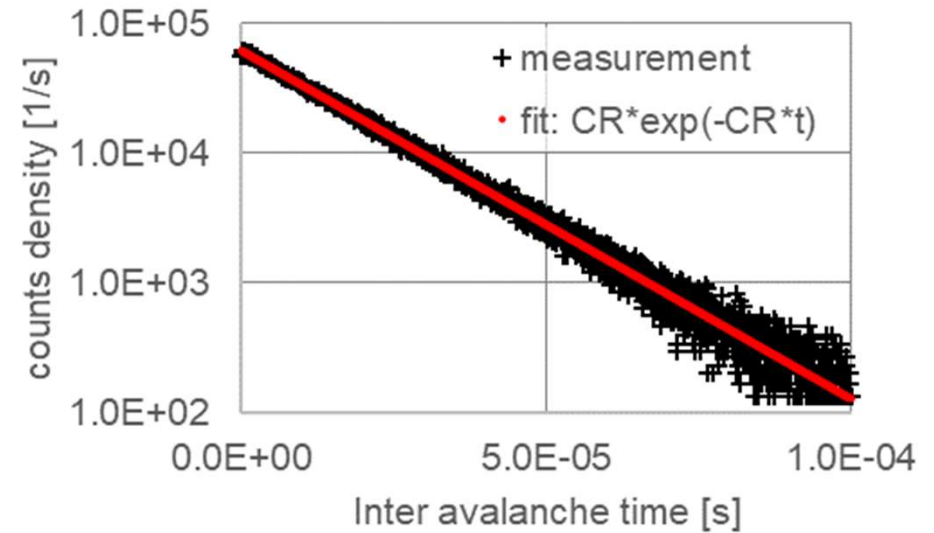
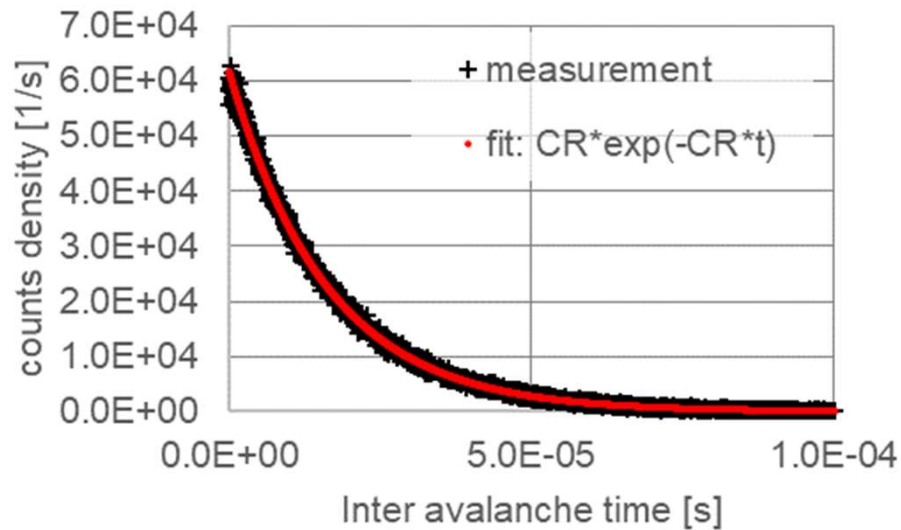
FF	FWHM	FW@10%	FW@1%
0.25	120	260	630
0.32	130	270	650
0.36	140	290	640
0.40	150	320	680
0.44	140	310	660
0.48	145	310	790
0.52	140	300	830

- Good jitter characteristics at 940nm!



After Pulsing Probability

25°C, $V_{exc}=3.0V$



- After pulsing probability is measured by the inter-avalanche time method.
- Measurement taken with 7ns dead time and low light condition.
- After pulsing probability < 0.5%

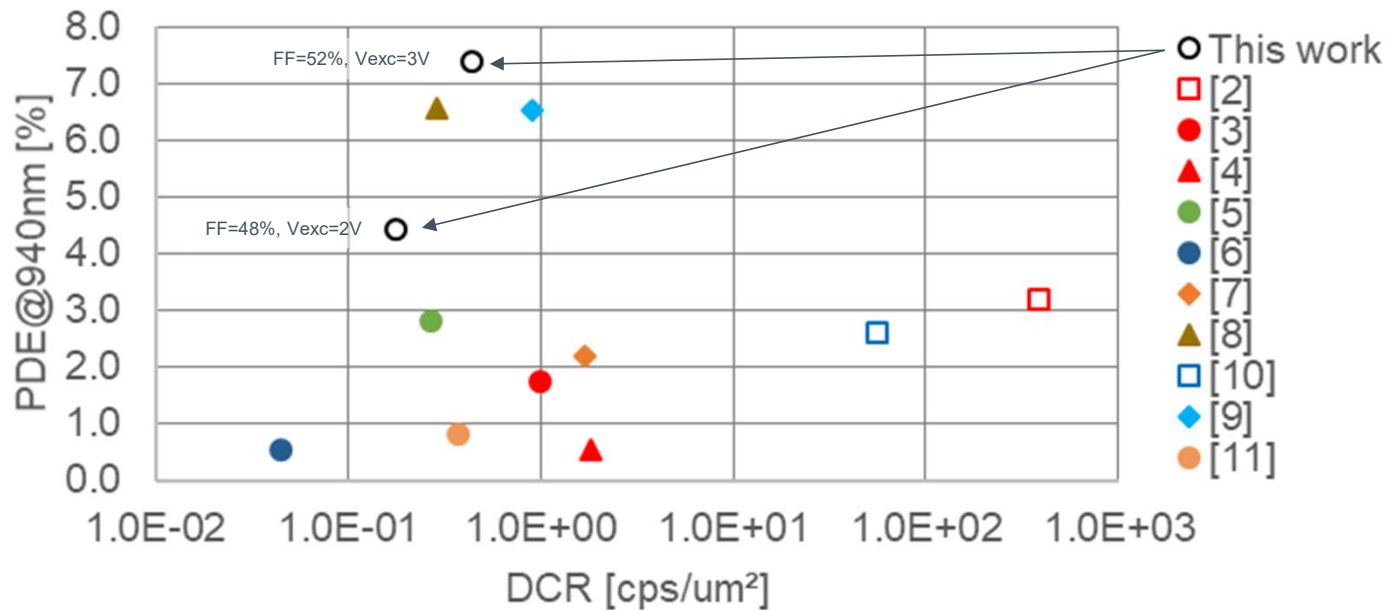
Performance Table

Typical parameters at 2V excess bias voltage, FF=0.48



Key Performance Indicator	Unit	Stacked BSI 45/40nm
Pixel pitch	um	~12.5
Breakdown voltage	V	17.0
DCR (25°C)	cps	14
DCR (75°C)	cps	270
PDE at 940nm	%	4.5
Timing jitter FWHM at 940nm	ps	145
Timing jitter (FW10%M) at 940nm	ps	310
Timing jitter (FW1%M) at 940nm	ps	790
After pulsing probability at 7ns dead time	%	<0.5
Cross talk probability	%	0.8

Benchmark



[1] This work
 [2] S. Lindner et al., "A High-PDE, Backside-Illuminated SPAD in 65/40-nm 3D IC CMOS Pixel With Cascoded Passive Quenching and Active Recharge", IEEE EDL vol. 38, no. 11, November 2017
 [3] S. Pellegrini et al., "Industrialized SPAD in 40nm Technology", IEDM 2017
 [4] S. Pellegrini et al., "Fully industrialized single photon avalanche diodes", SPIE proceedings vol. 10212, May 2017
 [5] I. Takai et al., "Single-Photon Avalanche Diode with Enhanced NIR-Sensitivity for Automotive LIDAR Systems", Sensors 16, no. 4: 459
 [6] D. Bronzi, "Low-noise and large-area CMOS SPADs with timing response free from slow tails", ESSDERC 2012
 [7] A. Fenigstein, "CMOS 0.18um SPAD", ISSW 2018
 [8] A. Gulinatti et al., "Improving the performance of silicon single-photon avalanche diodes", SPIE proceedings vol. 803302, May 2011
 [9] A. Gola, "NUV-HD and NIR-HD SiPMs and Applications", ISSW 2018
 [10] M. Lee et al., "High-Performance Back-Illuminated Three-Dimensional Stacked Single-Photon Avalanche Diode Implemented in 45-nm CMOS Technology", IEEE Journal of Selected Topics in Quantum Electronics, vol. 24, issue 6, Nov.-Dec. 2018
 [11] M. Morimoto et al., "High fill-factor miniaturized SPAD arrays with a guard-ring-sharing technique", Optics Express, vol. 28, issue 9, 2020



Thank you!

Please visit our website
www.ams.com